Transneuronal interactions facilitate axonal compartment formation

Authors: Bavat Bornstein[1], Idan Alyagor[1], Victoria Berkun[1], Hagar Meltzer[1], Fabienne Reh[2], Hadas Keren-Shaul[3,4], Eyal David[3], Thomas Riemensperger[2] and Oren Schuldiner[1]*

[1]Department of Molecular Cell Biology, Weizmann Institute of Sciences, Rehovot, Israel

[2]Department for Animal Physiology, Institute for Zoology, Biocenter Cologne, University of Cologne, Cologne, Germany

[3]Department of Immunology, Weizmann Institute of Sciences, Rehovot, Israel

[4]Life Science Core Facility, Weizmann Institute of Sciences, Rehovot, Israel

* Corresponding Author: oren.schuldiner@weizmann.ac.il

Abstract:

Precise connectivity of neurites to subcellular domains is a conserved feature of complex circuits, but the mechanisms defining precise wiring are largely unknown. The Drosophila mushroom-body is uniquely poised to study subcellular wiring as the adult γ-lobe harbors five distinct compartments, defined by localized innervations of other neuronal populations. Here we identify mechanisms required for precise wiring of γ-axons: Dpr12 and its interacting protein DIP-δ are both enriched at the γ4/5 compartments. However, while Dpr12 is cell-autonomously required in γ-neurons, DIP-δ acts in dopaminergic neurons for the formation of the γ4/5 compartments and the correct network architecture. Furthermore, γ-axons grow into regions preoccupied by DIP-δ+ neurons suggesting that they innervate a prepatterned lobe. Thus, transneuronal interactions that mediate precise wiring are required for axon compartmentalization.

One Sentence Summary:

Transneuronal interactions instruct precise wiring that enables localized innervation by specific neurons to distinct axonal compartments.

Main Text:

Accurate targeting of axons and dendrites is critical for circuit formation and function. Precise targeting is required to establish synapses not only at the correct target cell, but also at specified axodendritic domains (*1, 2*). For example, distinct neurons that innervate Pukinje cells, form synapses at distal or proximal dendritic spines, at dendritic shafts, or at the somata and axon initial segments (AIS). A gradient of the immunoglobulin superfamily (IgSF) protein Neurofascin, within the Purkinje cells, can drive basket cell targeting to the somata and AIS (*3*). Similarly, the L1 cell adhesion molecule (L1CAM) helps target chandelier neurons to the AIS of pyramidal neurons (*4*). While IgSF molecules define the AIS in both of these neuronal types, the identity of the interacting protein on the targeting neuron and thus the molecular mechanisms that underlie trans-recognition on both pre- and post-synaptic cells remain largely unknown. Given its unique development, connectivity and function, the *Drosophila* mushroom body (MB), offers an attractive model to study the mechanisms of precise targeting and formation of specific axonal domains. The adult MB, implicated in associated learning (*5-8*), is comprised of three major types of intrinsic neurons, γ, α'/β' and α/β, collectively known as Kenyon Cells (KCs). KCs form well-defined circuits with MB extrinsic neurons, which include MB output neurons (MBONs) and modulatory neurons, mostly dopaminergic (DANs). These MB extrinsic neurons innervate the KC axonal lobes in distinct locations to form discrete compartments (*9, 10*). For example, the γ-lobe is divided into five distinct axonal compartments termed γ1-γ5, defined by stereotypic inputs from specific DANs and MBONs (Fig. 1A). Importantly, these compartments have distinct functional roles. The γ1-γ2 compartments are associated with aversive memory, while the γ4-5 compartments participate in appetitive memory (*9, 11*). Yet, the mechanisms that control MB compartment formation remain unknown.

The γ-lobe undergoes extensive remodeling during development (*12*) (fig. S1A). We have previously demonstrated that regrowth of the adult γ lobe is genetically controlled by the nuclear receptor Unfulfilled (UNF) functioning as a ligand dependent transcription factor (*13*). To identify potential genes and pathways that mediate axon regrowth and targeting, we sequenced WT γ-neurons during development (*14*) alongside γ-neurons expressing UNF RNAi (Table S1). The expression of Ig superfamily (IgSF) encoding genes was dramatically affected ($p=3*10^{-29}$) by UNF-RNAi. Due to their dynamic expression, we focused on the Dpr/DIP families (fig. S1 and table S1). Knocking down (KD) *dpr12* by RNAi or by tissue specific (ts)CRISPR (*15-17*) in γ neurons induced a dramatic defect, where axons did not occupy the distal portion of the lobe (Fig. 1B-E).

Next, we generated a CRISPR mediated a *dpr12* loss of function mutant (*dpr12*$^{\Delta 50\text{-}81}$, fig. S2). At 3rd instar larva (L3), γ-neurons in *dpr12*$^{\Delta 50\text{-}81}$ homozygotes exhibited WT morphology (Fig. 1F, J) and subsequently pruned normally (data not shown). In contrast γ neurons in *dpr12*$^{\Delta 50\text{-}81}$ animals failed to extend to the distal part of the lobe at 48h APF, a time when γ axons normally have completed their regrowth (*12, 18*), and in adult (Fig. 1G, H, K, L). Importantly, γ specific

expression of a *Dpr12* transgene fully rescued the regrowth defect within *dpr12*$^{\Delta 50\text{-}81}$ homozygotes (Fig. 1I, M, N, ranking examples shown in fig. S3).

To determine whether Dpr12 functions in a cell-autonomous manner, we used the Mosaic Analysis with a Repressible Cell Marker (MARCM) technique to express *dpr12-RNAi* within neuroblast (NB) or single cell (SC) clones. We found that both NB and SC clones expressing *dpr12* RNAi exhibited normal growth at L3 but failed to fully extend axons at 48hr APF and in adult flies (Fig. 1O-R, fig S4). Because the γ-lobe is divided into distinct compartments we next mapped the premature stopping in more detail. We measured the length of adult WT and mutant axons relative to the γ-lobe span and superimposed these data onto the γ compartments, as defined by distinct innervations of MBONs and DANs (Fig. 1S, fig. S5)(*9, 19*). We conclude that Dpr12 is cell-autonomously required for γ-neuron projection into the γ4/5 compartments. To the best of our knowledge, this is the first report of a cell-autonomous role for Dpr proteins.

To assess Dpr12 protein localization, we used the *Minos* Mediated Integration Cassette (MiMIC)(*20*) transgene collection to generate a GFP insertion within the endogenous *Dpr12* locus, which should produce a Dpr12-GFP fusion protein (*21*) (Dpr12^{GFSTF}; fig. S2). We found that Dpr12-GFP localized to the distal part of γ-axons at L3 (Fig. 2A), then it became diffused at 24hr APF, when γ-axons initiate their developmental regrowth (Fig. 2B). Finally, at 48h APF and in adulthood, Dpr12 relocalized to the distal part of the lobe (Fig. 2C-D) and was restricted to the adult γ4 and γ5 compartments (Fig. 2D). Our data suggest that Dpr12 is expressed at the right time and place to mediate γ-axon regrowth into the γ4/γ5 compartments.

Dprs can form heterophilic interactions with DIPs in a rather promiscuous fashion, in which most Dprs can bind to multiple DIPs and most DIPs can bind to multiple Dprs (*22-24*). Interestingly, Dpr12 and DIP-δ represent a unique case of 'monogamous' binding. We found that DIP-δ-GFP (DIP-δ^{GFSTF}; fig. S6) localized, similarly to Dpr12, to the γ4/5 compartments (Fig. 2H). However, in contrast to Dpr12, DIP-δ was localized to the distal MB lobe throughout development (Fig. 2E-H), including at 24hr APF, when γ-axons are completely pruned and have not yet extended (Fig. 2F). Taken together, these data indicate that DIP-δ is localized to γ4/γ5 compartments throughout development and is expressed in cells that project to this region before γ neurons reach their terminal projections.

We next asked whether DIP-δ is also required for regrowth of γ-neurons into the γ4/5 compartments. We therefore both generated and obtained *DIP-δ* mutant alleles (*DIP-δ*$^{T2A\text{-}Gal4}$, *DIP-δ*$^{1\text{-}119}$, respectively; fig. S6). *DIP-δ* homozygous and trans-heterozygous combinations were viable, enabling us to mark γ-neurons by a membrane bound Tomato (QUAS-mtdT-3XHA) driven by a Gal4 independent binary system driver (71G10-QF2). At L3, γ-neurons within *DIP-δ* mutant brains exhibited WT morphology (Fig. 3A, E), indicating that DIP-δ is not required for their initial axon extension. However, *DIP-δ* mutant brains displayed a γ-axon regrowth defect at 48hr APF, and in adult (Fig. 3B, C, F, G, fig. S7) which resembled the *dpr12* mutant phenotype. To confirm that *DIP-δ* loss-of-function induced this γ-axon regrowth defect, we exploited the fact that the *DIP-δ*$^{T2A\text{-}Gal4}$ allele also expresses Gal4 in DIP-δ^{+} neurons (fig. S6). Expressing *DIP-*

δ transgene driven by *DIP-δ$^{T2A-Gal4}$* rescued the γ-neuron regrowth defect (Fig. 3D, H, I) indicating that DIP-δ is required for γ-neuron innervation of the γ4/5 compartments.

Our data suggest that DIP-δ is expressed in extrinsic MB neurons that innervate the γ4/γ5 compartments (fig. S8). These compartments are strongly innervated by the Protocerebral Anterior Medial (PAM) neurons, a population of about 100 DANs, as well as by specific groups of MBONs (*9, 10*). To investigate whether DIP-δ is expressed in these cells, we selectively ablated PAMs or MBONs by cell type specific expression of Diphtheria toxin (UAS-DTI) and assayed DIP-δ-GFP localization. Ablating γ4 MBONs using multiple Gal4s (see materials and methods) did not affect DIP-δ expression (fig. S9). In contrast, ablating PAM DANs using R58E02-Gal4 drastically reduced γ4/5 specific DIP-δ expression (fig. S9). While we cannot exclude the possibility that DIP-δ is also expressed in other MBONs that innervate the γ4 compartment, these results strongly suggest that at the adult stage, γ4/γ5 DIP-δ protein is mainly, if not exclusively, expressed by PAM DANs, consistent with recent profiling experiments (*25*).

Next, we visualized PAM-DANs during development to determine if they may provide a template for γ-axon growth, as suggested by DIP-δ-GFP expression (Fig. 2). Since the 'classical' PAM driver, R58E02, is not expressed throughout development (fig. S10A-C), we analyzed the expression of *DIP-δ$^{T2A-Gal4}$* (fig. S10D-F) and then used the MARCM technique to label sparse *DIP-δ$^{T2A-Gal4}$* clones (Fig. 3J-L; of note, these clones remain heterozygous for DIP-δ). We detected DIP-δ expressing clones that innervate the γ4/γ5 compartments as early as 24hr APF throughout adulthood. Interestingly, these clones do not seem to express tyrosine hydroxylase (TH), required for Dopamine biogenesis, at 24hr APF but become TH positive at 48hr APF onwards. In summary, our data suggest that DIP-δ is expressed in PAM-DANs, which innervate the future γ4/5 compartments as early as 24hr APF, and support the speculation that DIP-δ expressed in PAM-DANs may provide a template for γ-axon growth.

Both Dpr12 and DIP-δ localize to the γ4/5 compartments and are required for their formation likely by mediating interactions between γ-neurons and PAM-DANs. We therefore investigated how losing either *dpr12* or *DIP-δ* affects their binding partner localization and mature circuit architecture. First, we investigated whether the highly localized expression of Dpr12 and DIP-δ is cell-autonomous or requires interaction with their binding partner. We visualized Dpr12 and DIP-δ GFP fusion proteins in brains homozygous mutant for their reciprocal Dpr/DIP partner. We found that Dpr12 expression appears diffuse in *DIP-δ* mutant brains throughout development (fig. S11), indicating that Dpr12 protein localization requires interaction with DIP-δ, likely on PAM-DANs. In contrast, DIP-δ localization did not dramatically change during the early stages of development in *dpr12* mutants (fig. S11). At 48hr APF, while we still detected DIP-δ at the distal part of the lobe, it occupied a smaller area than in WT brains and resembled the innervation pattern typical of 24hr APF (compare fig. S11G to Fig. 2G). We did not detect any DIP-δ in the adult MB medial lobe (fig. S11H). Together, these results indicate that while DIP-δ is required for Dpr12 localization throughout development, Dpr12 is required only for maintenance of the adult localization of DIP-δ.

We next determined if the loss of normal Dpr12-DIP-δ interaction induced axonal misrouting, cell loss or other circuit reorganizations. We found that, in *dpr12* mutants, γ4 or γ5 PAM-DANs misrouted and failed to form substantial connections within the γ-lobe (Fig. 4A-D, fig. S12). Importantly, the number of PAM-DANs remained unchanged (fig. S12C, F). In contrast, γ4-MBON still innervated the γ-lobe in *dpr12* mutant brains, albeit in abnormal locations like the γ3 compartment (Fig. 4E-F, fig. S12). Finally, we examined the global neuropil structure in *dpr12* mutant brains by following staining of the active zone protein bruchpilot (Brp) which demonstrated that the γ4/5 compartments were largely missing (Fig. 4G-H, Movies S1-2). Interestingly, the lack of these domains is accompanied by enlarged γ2/3 compartments, as well as distortions in other brain regions (see Crepine, for example, in Fig. 4G-H).

How axons and dendrites target and subsequently form sub-neurite domains is not well understood. Using the unique development and morphology of the *Drosophila* MB, we identify a molecular mechanism that mediates the formation of distinct axonal compartments. To the best of our knowledge, this is the first identification of molecules functioning at both the pre- and post-synaptic neurons that mediate wiring and formation of axonal compartments.

We show that the interaction between Dpr12 on γ neurons and DIP-δ on PAM-DANs underlies the formation of MB γ4/5 compartments. The discrete and non-overlapping compartments of the adult γ lobe, as well as other MB lobes, are defined by the specific innervations of other neurons. Within each compartment, input from DANs can modify synaptic strength between the KC and MBON. Importantly, these compartments are functionally distinct (*9, 11, 26, 27*). Based on our data, we speculate that various specific combinations of adhesion molecules mediate target recognition events that occur between predefined pre- and post-synaptic pairs in other compartments. γ-neurons express a broad spectrum of IgSFs in tight temporal regulation, highlighting their potential role in circuit formation (*14*). However, many adhesion molecules, including Dpr/DIPs, can form promiscuous interactions making their analyses challenging. Future studies could use CRISPR/Cas9 technology to generate multi-gene mutations to further explore the adhesion code required for compartment formation.

Expression patterns of Dpr and DIP molecules in the neuromuscular junction (NMJ) (*22*) and visual system (*22, 28*) suggested a model where these molecules instruct target cell specificity. Recent loss-of-function experiments strengthened this target specificity hypothesis as the DIP-α-Dpr10 interaction was shown to be important for motoneuron innervation of specific larval (*29*) and adult (*30*) muscles and DIP-α-Dpr10/Dpr6 interaction for specific layer targeting in the visual system (*31*). Our results suggest that mechanisms used to target axons and dendrites to specific cell types or layers may be further implicated to orchestrate the formation of axonal compartment. Pairwise IgSF molecular interactions are conserved in vertebrates and invertebrates (*32, 33*) implying similar mechanisms for the formation subcellular compartments in other organisms.

References and Notes:

1. J. R. Sanes, M. Yamagata, Many paths to synaptic specificity. *Annual review of cell and developmental biology* **25**, 161-195 (2009).
2. J. de Wit, A. Ghosh, Specification of synaptic connectivity by cell surface interactions. *Nature reviews. Neuroscience* **17**, 22-35 (2016).
3. F. Ango *et al.*, Ankyrin-based subcellular gradient of neurofascin, an immunoglobulin family protein, directs GABAergic innervation at purkinje axon initial segment. *Cell* **119**, 257-272 (2004).
4. Y. Tai, N. B. Gallo, M. Wang, J. R. Yu, L. Van Aelst, Axo-axonic Innervation of Neocortical Pyramidal Neurons by GABAergic Chandelier Cells Requires AnkyrinG-Associated L1CAM. *Neuron* **102**, 358-372 e359 (2019).
5. M. Heisenberg, Mushroom body memoir: from maps to models. *Nature reviews. Neuroscience* **4**, 266-275 (2003).
6. B. Gerber *et al.*, Visual learning in individually assayed Drosophila larvae. *J Exp Biol* **207**, 179-188 (2004).
7. A. Fiala, Olfaction and olfactory learning in Drosophila: recent progress. *Current opinion in neurobiology* **17**, 720-726 (2007).
8. D. Owald, S. Waddell, Olfactory learning skews mushroom body output pathways to steer behavioral choice in Drosophila. *Current opinion in neurobiology* **35**, 178-184 (2015).
9. Y. Aso *et al.*, The neuronal architecture of the mushroom body provides a logic for associative learning. *eLife* **3**, e04577 (2014).
10. N. K. Tanaka, H. Tanimoto, K. Ito, Neuronal assemblies of the Drosophila mushroom body. *J Comp Neurol* **508**, 711-755 (2008).
11. P. Cognigni, J. Felsenberg, S. Waddell, Do the right thing: neural network mechanisms of memory formation, expression and update in Drosophila. *Current opinion in neurobiology* **49**, 51-58 (2018).
12. T. Lee, A. Lee, L. Luo, Development of the Drosophila mushroom bodies: sequential generation of three distinct types of neurons from a neuroblast. *Development* **126**, 4065-4076 (1999).
13. S. P. Yaniv, N. Issman-Zecharya, M. Oren-Suissa, B. Podbilewicz, O. Schuldiner, Axon regrowth during development and regeneration following injury share molecular mechanisms. *Current biology : CB* **22**, 1774-1782 (2012).
14. I. Alyagor *et al.*, Combining Developmental and Perturbation-Seq Uncovers Transcriptional Modules Orchestrating Neuronal Remodeling. *Developmental cell* **47**, 38-52 e36 (2018).
15. F. Port, S. L. Bullock, Augmenting CRISPR applications in Drosophila with tRNA-flanked sgRNAs. *Nature methods* **13**, 852-854 (2016).

16. F. Port, H. M. Chen, T. Lee, S. L. Bullock, Optimized CRISPR/Cas tools for efficient germline and somatic genome engineering in Drosophila. *Proceedings of the National Academy of Sciences of the United States of America* **111**, E2967-2976 (2014).
17. H. Meltzer *et al.*, Tissue-specific (ts)CRISPR as an efficient strategy for in vivo screening in Drosophila. *Nature communications* **10**, 2113 (2019).
18. D. Rabinovich, S. P. Yaniv, I. Alyagor, O. Schuldiner, Nitric Oxide as a Switching Mechanism between Axon Degeneration and Regrowth during Developmental Remodeling. *Cell* **164**, 170-182 (2016).
19. Y. Shuai *et al.*, Dissecting neural pathways for forgetting in Drosophila olfactory aversive memory. *Proceedings of the National Academy of Sciences of the United States of America* **112**, E6663-6672 (2015).
20. K. J. Venken *et al.*, MiMIC: a highly versatile transposon insertion resource for engineering Drosophila melanogaster genes. *Nature methods* **8**, 737-743 (2011).
21. S. Nagarkar-Jaiswal *et al.*, A library of MiMICs allows tagging of genes and reversible, spatial and temporal knockdown of proteins in Drosophila. *eLife* **4**, (2015).
22. R. A. Carrillo *et al.*, Control of Synaptic Connectivity by a Network of Drosophila IgSF Cell Surface Proteins. *Cell* **163**, 1770-1782 (2015).
23. E. Ozkan *et al.*, An extracellular interactome of immunoglobulin and LRR proteins reveals receptor-ligand networks. *Cell* **154**, 228-239 (2013).
24. F. Cosmanescu *et al.*, Neuron-Subtype-Specific Expression, Interaction Affinities, and Specificity Determinants of DIP/Dpr Cell Recognition Proteins. *Neuron* **100**, 1385-1400 e1386 (2018).
25. V. Croset, C. D. Treiber, S. Waddell, Cellular diversity in the Drosophila midbrain revealed by single-cell transcriptomics. *eLife* **7**, (2018).
26. Y. Aso *et al.*, Mushroom body output neurons encode valence and guide memory-based action selection in Drosophila. *eLife* **3**, e04580 (2014).
27. R. Cohn, I. Morantte, V. Ruta, Coordinated and Compartmentalized Neuromodulation Shapes Sensory Processing in Drosophila. *Cell* **163**, 1742-1755 (2015).
28. L. Tan *et al.*, Ig Superfamily Ligand and Receptor Pairs Expressed in Synaptic Partners in Drosophila. *Cell* **163**, 1756-1769 (2015).
29. J. Ashley *et al.*, Transsynaptic interactions between IgSF proteins DIP-alpha and Dpr10 are required for motor neuron targeting specificity. *eLife* **8**, (2019).
30. L. Venkatasubramanian *et al.*, Stereotyped terminal axon branching of leg motor neurons mediated by IgSF proteins DIP-alpha and Dpr10. *eLife* **8**, (2019).
31. S. Xu *et al.*, Interactions between the Ig-Superfamily Proteins DIP-alpha and Dpr6/10 Regulate Assembly of Neural Circuits. *Neuron* **100**, 1369-1384 e1366 (2018).
32. K. Zinn, E. Ozkan, Neural immunoglobulin superfamily interaction networks. *Current opinion in neurobiology* **45**, 99-105 (2017).
33. S. L. Zipursky, J. R. Sanes, Chemoaffinity revisited: dscams, protocadherins, and neural circuit assembly. *Cell* **143**, 343-353 (2010).

34. D. Kim, B. Langmead, S. L. Salzberg, HISAT: a fast spliced aligner with low memory requirements. *Nature methods* **12**, 357-360 (2015).
35. M. I. Love, W. Huber, S. Anders, Moderated estimation of fold change and dispersion for RNA-seq data with DESeq2. *Genome Biol* **15**, 550 (2014).
36. S. Heinz *et al.*, Simple combinations of lineage-determining transcription factors prime cis-regulatory elements required for macrophage and B cell identities. *Molecular cell* **38**, 576-589 (2010).
37. J. P. Vert, N. Foveau, C. Lajaunie, Y. Vandenbrouck, An accurate and interpretable model for siRNA efficacy prediction. *BMC Bioinformatics* **7**, 520 (2006).
38. S. J. Gratz *et al.*, Highly specific and efficient CRISPR/Cas9-catalyzed homology-directed repair in Drosophila. *Genetics* **196**, 961-971 (2014).
39. F. Diao *et al.*, Plug-and-play genetic access to drosophila cell types using exchangeable exon cassettes. *Cell Rep* **10**, 1410-1421 (2015).
40. T. Lee, L. Luo, Mosaic analysis with a repressible cell marker for studies of gene function in neuronal morphogenesis. *Neuron* **22**, 451-461 (1999).

Acknowledgments:

We thank Larry Zipursky for sharing unpublished reagents, the Bloomington Stock Centers for reagents; monoclonal antibodies were obtained from the Developmental Studies Hybridoma Bank developed under the auspices of the NICHD and maintained by the University of Iowa. We thank R. Rothkopf for assistance with statistics; M. Schuldiner, A. Yaron and the O.S lab for discussions and critical reading of this manuscript. We thank Life Science Editors for editing assistance. **Funding:** This work was supported by the European Research Council (erc), consolidator grant # 615906, "AxonGrowth". Fly food for this project was funded by the Women Health Research Center. O.S. is the Incumbent of the Prof. Erwin Netter Professorial Chair of Cell Biology, T.R. was supported by Axa as team member of the Axa Chair from genome to structure, F.R is a GSfBS member. **Competing interests:** Authors declare no competing interests. **Data and materials availability:** All data is available in the main text or the supplementary materials. In addition, RNAseq data will be available via Gene Expression Omnibus at NCBI.

Supplementary Materials:

Materials and Methods

Figures S1-S12

Tables S1-S2

Movies S1-S2

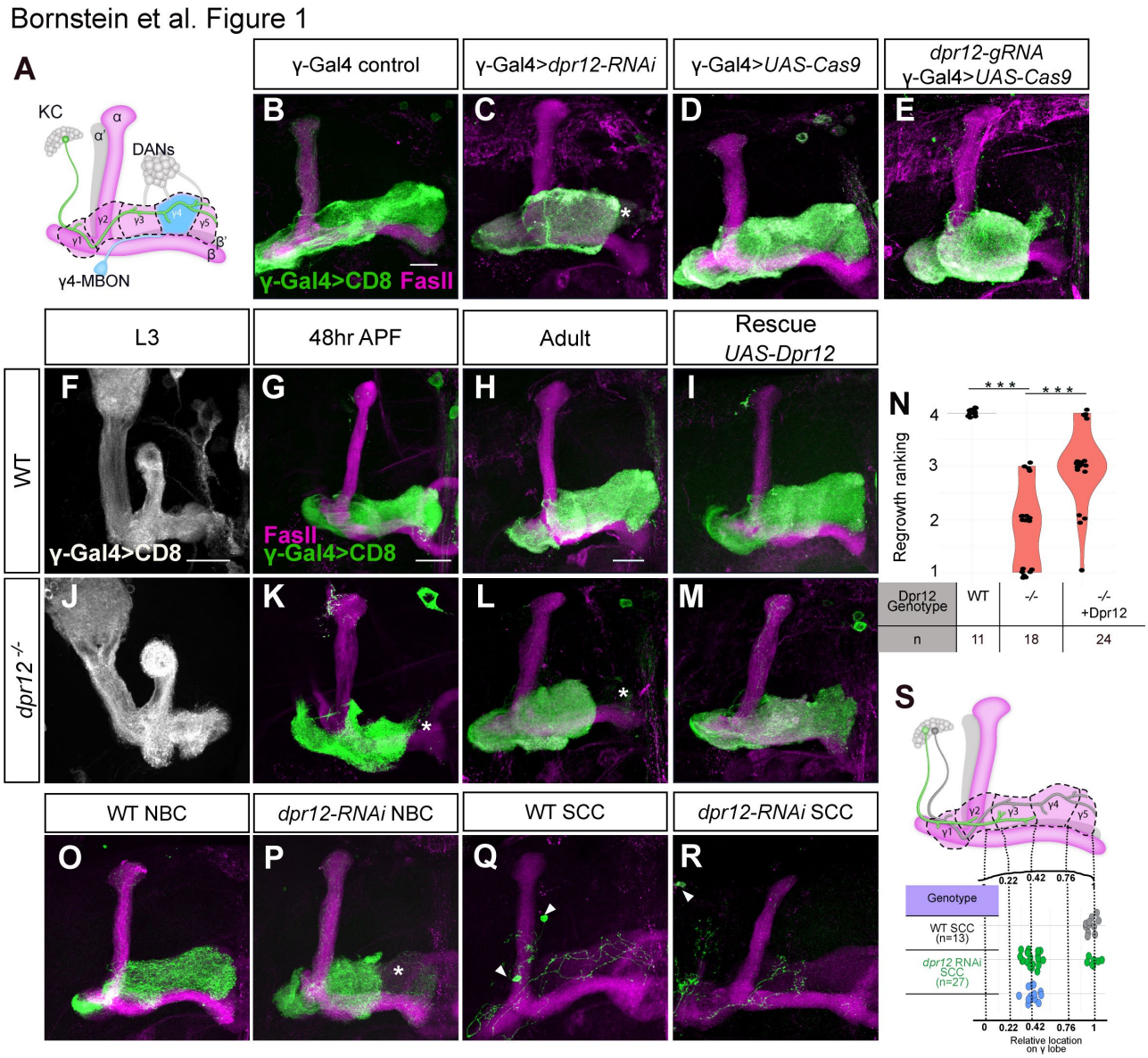

Fig. 1. Dpr12 is cell autonomously required for γ-neuron regrowth into the γ4/5 compartments

(A) Schematic representation of the adult MB and specific γ lobe compartments. Intrinsic MB neurons (also called Kenyon Cells; KC) form the α, α', β, β' and γ lobes. A single γ neurons is indicated in green, projecting into the γ lobe, which is divided into the γ1-γ5 compartments, which are defined by the stereotypic innervation by extrinsic MB neurons such as Dopaminergic (DANs, gray) and MB output neurons (MBONs). An example of a γ4 MBON is shown in cyan.

(B-M) Confocal z-projections of the indicated genotypes and age labeled with membrane bound GFP (mCD8-GFP; CD8) driven by the γ specific Gal4 driver R71G10-Gal4 (γ-Gal4). While γ neurons of control flies project through the entire lobe (B; n=12/12, D; n=14/14), knockdown of

dpr12 by RNAi (C; n=12/12) or knockout by tsCRISPR (E; n=14/14) resulted in short axons. At L3, γ neurons within *dpr12*$^{\Delta 50\text{-}81}$ homozygotes (J; n=20/20) resemble WT (F; n=20/20). At 48h APF, WT γ neurons (G; n=12/12) re-extend their axons to form the adult lobe, while *dpr12*$^{\Delta 50\text{-}81}$ γ neurons (K; n=14/14) fail to extend their axons fully. This defect persists to adulthood (H; n=11/11, L; n=18/18). Expressing a *UAS-Dpr12* transgene within γ neurons in *dpr12*$^{\Delta 50\text{-}81}$ homozygotes rescued the axon regrowth defect (M; n=23/24, I; n=14/14).

(N) Quantification of the regrowth defects in H, L and M. The z-projections were blindly classified into four classes of regrowth defect severity (see fig. S3). Kruskal-Wallis test followed by a Mann-Whitney post-hoc test determined significance; ***$p<0.001$.

(O-R) Confocal z-projections of MARCM neuroblast clone (NBC) and single-cell clones (SCC) labeled with membrane bound GFP (mCD8-GFP; CD8) driven by the γ specific Gal4 driver 71G10-Gal4 (γ-Gal4). WT clones (O; n=10/10, Q; n=13/13) extend their axons to form the full adult lobe, while clones expressing *dpr12* RNAi (P; n=18/24, R; n=19/27) fail to extend fully.

(S) Measurements of WT (Q) and *dpr12* RNAi (R) SCC growth into the γ-lobe superimposed onto the distinct γ compartments, as measured in fig. S5.

Asterisks demarcate the distal part of the lobe, arrowheads demarcate single cell bodies. Green and white represent mCD8-GFP. Magenta shows FasII. Scale bar is 20µm.

Bornstein et al. Figure 2

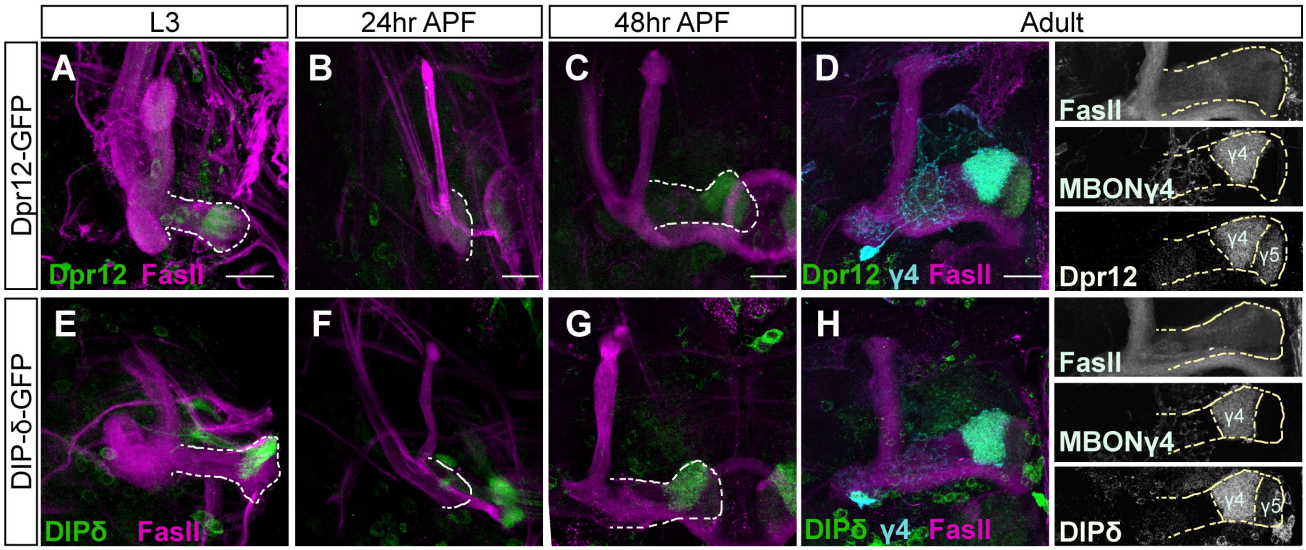

Fig. 2. Dpr12 and its interacting protein DIP-δ localize to the γ4/5 compartments

(A-H) Confocal z-projections of brains expressing MiMIC mediated Dpr12^{GFSTF} (Dpr12-GFP) and DIP-δ^{GFSTF} (DIP-δ-GFP) fusion proteins at the indicated timepoints. See fig. S1 and S3 for more details.

(A-D) Dpr12-GFP is localized to the distal part of the γ lobe at L3 (A; n=10/10), 48hr APF (C; n=12/12) and the adult stage (D; n=20/20), where it colocalizes with a γ4 MBON (γ4; labeled by R18H09-Gal4 driving the expression of CD4-tdT). At 24hr APF (B; n=10/10), Dpr12-GFP appears diffuse.

(E-H) DIP-δ-GFP is localized to the distal part of the γ lobe throughout development: L3 (E; n=16/16), 24hr APF (F; n=10/10), 48hr APF (G; n=12/12) and adult (H; n=24/24), where it colocalizes with a γ4 MBON.

Dashed line depicts the medial γ axonal lobe. Green is GFP, cyan is CD4-tdT, magenta is FasII. Grayscale in D and H represent single channels, as marked. Scale bar is 20µm.

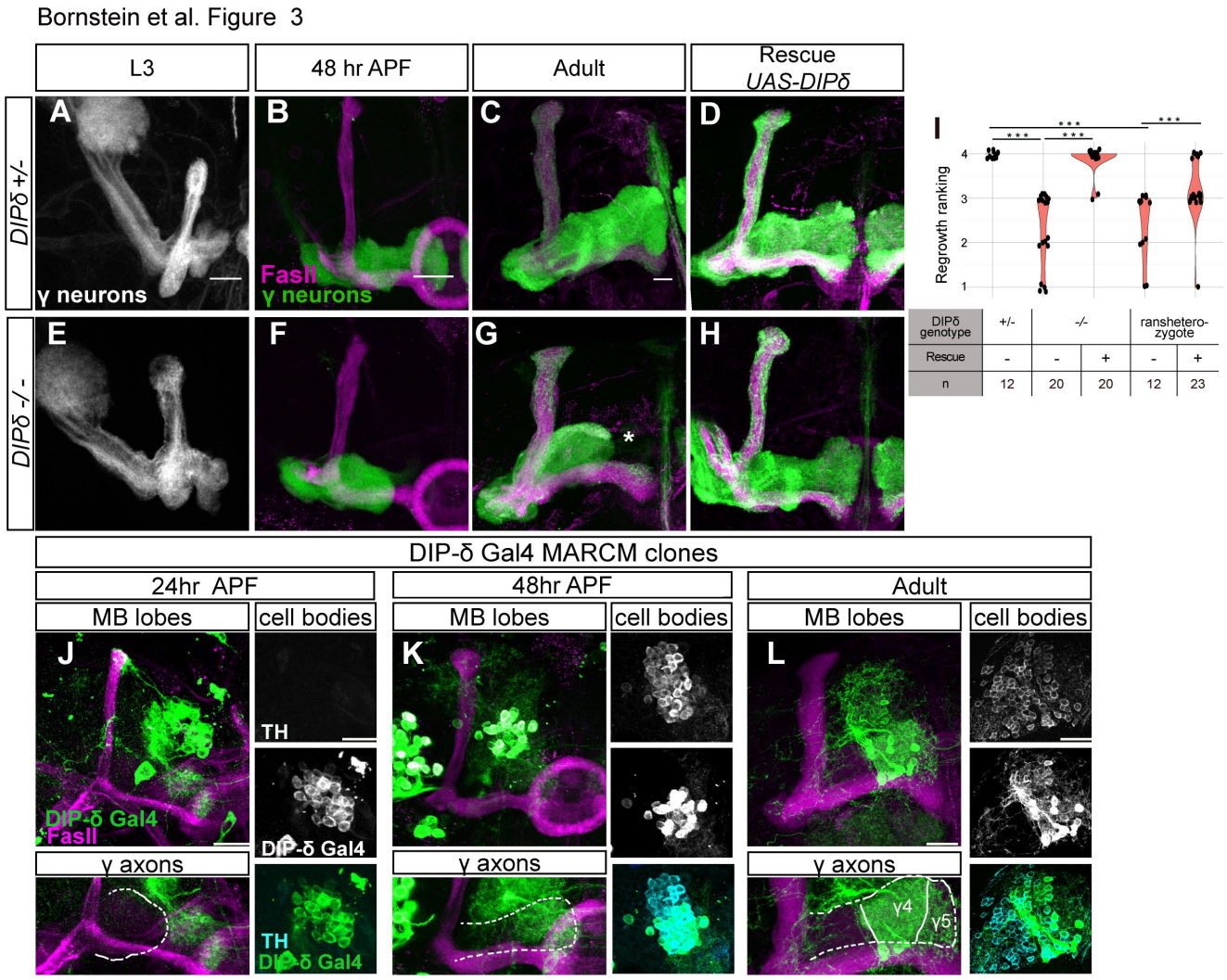

Fig. 3. DIP-δ is required for γ-neuron regrowth into the γ4/5 compartments

(A-H) Confocal z-projections *DIP-δ* hetero- and homozygous brains in which γ neurons were labeled by expressing membrane bound tandem tomato (mtdT-HA) driven by the γ specific QF2 driver R71G10-QF2 (γ-neurons). Larval (L3) γ neurons grow normally in *DIP-δ*$^{T2A\text{-}Gal4}$ heterozygotes (A; n=16/16) and homozygotes (E; n=24/24). In contrast, at 48hr APF and adult, γ neurons within *DIP-δ*$^{T2A\text{-}Gal4}$ homozygotes do not enter the distal part of the lobe (asterisks; F; n=8/8, G; n=20/20), while they grow normally in heterozygotes (B; n=12/12, C; n=12/12). Overexpression of a *DIP-δ* transgene driven by the Gal4 activity of *DIP-δ*$^{T2A\text{-}Gal4}$ (see fig. S5) does not affect normal growth (D; n=10/10) and rescues mutant phenotypes (H; n=20/20). Asterisks demarcate distal part of the lobe. Green and white are mtdT-HA, magenta is FasII, Scale bar is 20µm.

(I) Quantification of the regrowth defects in C, D, G, H, and fig. S7. Regrowth defect severity and statistics were calculated as in Fig. 1; ***p<0.001

(J-L) Confocal z-projections of MARCM clones labeled by *DIP-δ*$^{T2A\text{-}Gal4}$ (DIP-δ Gal4) driving the expression of membrane bound GFP (mCD8-GFP; CD8) and heat shocked at 24hr after egg laying. Clones innervate the γ4/γ5 domains at 24hr APF (J; n=8), 48hr APF (K; n=8) and adult (L; n=16). Clones become tyrosine hydroxylase (TH) positive only at 48hr APF onwards. Magenta is FasII, green is mCD8-GFP, cyan is TH antibody staining, grayscale single channels are shown as indicated. Scale bar is 20µm.

Bornstein et al. Figure 4

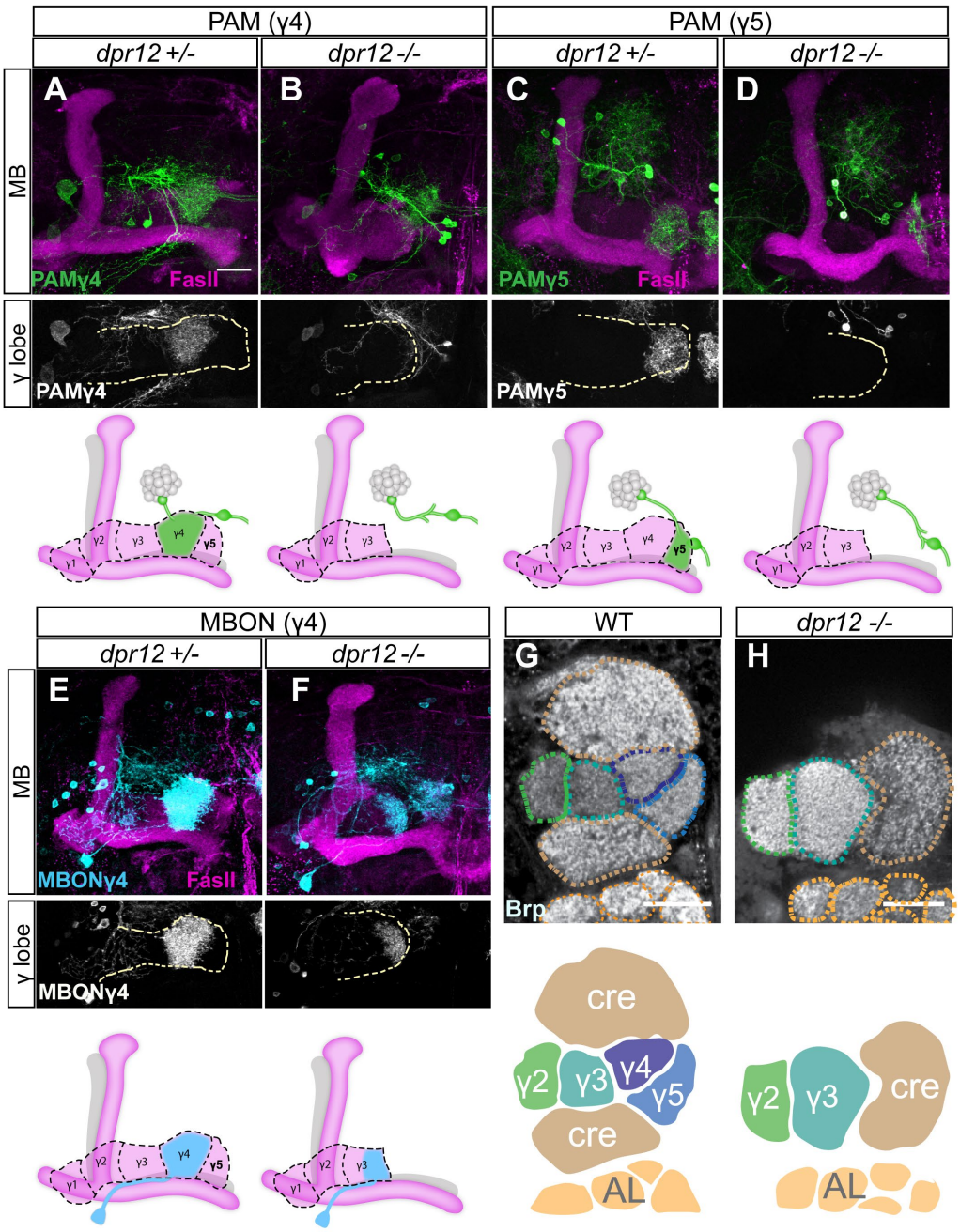

Fig. 4. Dpr12-DIP-δ interaction mediates circuit assembly

(A-F) Confocal z-projections of *dpr12*$^{\Delta 50\text{-}81}$ heterozygous (A, n=15; C, n=10; E, n=10) and homozygous brains (B, n=8; D, n=18; F, n=24) expressing mCD8-GFP (CD8) driven by: (A-B) R10G03-Gal4 (PAMγ4); (C-D) R48H11-Gal4 (PAMγ5), or (E-F) R18H09-Gal4 (MBONγ4). Schematics shown below summarize MB lobe structure in different *dpr12* genotypes.

(G-H) Single confocal slices of WT (G, n=5/5) and *dpr12*$^{\Delta 50\text{-}81}$ homozygous brains (H, n=5/5) stained with anti-Brp. Dashed lines demarcate neuropil boundaries, schematic shown below. cre,

crepin; AL, antenna lobe.

Magenta is FasII, green and cyan are mCD8-GFP, grayscale depicts single channels as indicated. Scale bar is 20µm.

5